2016

Characterisation of silicon diode arrays for dosimetry in external beam radiation therapy

Claudiu S. Porumb
University of Wollongong, csp528@uowmail.edu.au

Abdullah H. Aldosari
University of Wollongong, ahaa215@uowmail.edu.au

Iolanda Fuduli
University of Wollongong, if473@uowmail.edu.au

Dean L. Cutajar
University of Wollongong, deanc@uow.edu.au

Matthew Newall
University of Wollongong, mkn282@uowmail.edu.au

See next page for additional authors

Characterisation of silicon diode arrays for dosimetry in external beam radiation therapy

Abstract

Modern stereotactic radiation therapy modalities utilize small beams and large dose gradients to deliver radiation in few fractions, reducing the possibility to correct for mistakes during the treatment process. Therefore, in order to ensure best possible treatment for the patient, quality assurance for such treatments necessitates a stable, linear, and sensitive radiation detector with high spatial resolution and radiation hardness. In this work, two silicon detector arrays with high spatial resolution have been characterized by 6 MV and 18 MV medical LINAC irradiation, and 5.5 MeV He2+ heavy ion microprobe. A maximum discrepancy of 0.6 mm in field size has been found when comparing to two-dimensional radiochromic film dose profile, and charge collection efficiency obtained by means of ion beam induced charge collection (IBICC) is 66% when operating the array in photovoltaic mode. Radiation damage study by photons and photoneutrons is presented.

Disciplines

Engineering | Science and Technology Studies

Authors

Claudiu S. Porumb, Abdullah H. Aldosari, Iolanda Fuduli, Dean L. Cutajar, Matthew Newall, Peter E. Metcalfe, Martin G. Carolan, Michael L. F Lerch, Vladimir Perevertaylo, Anatoly B. Rosenfeld, and Marco Petasecca

Characterisation of Silicon Diode Arrays for Dosimetry in External Beam Radiation Therapy

Claudiu S. Porumb, Abdullah H. Aldosari, Iolanda Fuduli, Dean Cutajar, Matthew Newall, Peter Metcalfe, Martin Carolan, Michael L. F. Lerch, *Member, IEEE*, Vladimir L. Perevertaylo, Anatoly B. Rosenfeld, *Senior Member, IEEE*, and Marco Petasecca, *Member, IEEE*

Abstract—Modern stereotactic radiation therapy modalities utilize small beams and large dose gradients to deliver radiation in few fractions, reducing the possibility to correct for mistakes during the treatment process. Therefore, in order to ensure best possible treatment for the patient, quality assurance for such treatments necessitates a stable, linear, and sensitive radiation detector with high spatial resolution and radiation hardness. In this work, two silicon detector arrays with high spatial resolution have been characterized by 6 MV and 18 MV medical LINAC irradiation, and 5.5 MeV He^{2+} heavy ion microprobe. A maximum discrepancy of 0.6 mm in field size has been found when comparing to two-dimensional radiochromic film dose profile, and charge collection efficiency obtained by means of ion beam induced charge collection (IBICC) is 66% when operating the array in photovoltaic mode. Radiation damage study by photons and photoneutrons is presented.

Index Terms—Dosimetry, neutron radiation effects, silicon radiation detectors

I. INTRODUCTION

ACCORDING to the World Health Organization (WHO), the number of deaths from cancer is increasing and could reach 12 million by 2030 [1]. Some cancers, however, can be cured, or at least the suffering of patients minimized, if diagnosed and treated at early stage. The three most common options for treatment are chemotherapy, surgery and radiotherapy. Of all cured patients, 30% are treated with radiotherapy, and more than half of all patients receive radiotherapy as part of their cancer management plan [1][2]. The prime objective of radiation therapy is the effective delivery of ionizing radiation to a specific target, while avoiding surrounding healthy tissues [3]. Stereotactic Radiotherapy (SRT) is a delivery technology which has high dose conformation to the tumor volume while maximizing healthy tissue sparing. SRT includes Stereotactic Body Radiation Therapy (SBRT) and Stereotactic Radiosurgery (SRS).

The high hypo-fractionation regimes used in these techniques (up to 90 Gy delivered in 2 up to 5 fractions for SBRT and one single fraction for SRS) requires an accurate patient-specific Quality Assurance for verification of the plan [4].

Standard codes of practice for reference dosimetry [5][6] are based on broad radiation fields in which lateral electronic equilibrium is always conserved. SRT techniques involve small radiation fields where lateral electronic equilibrium is not conserved anymore, and partial blocking of the beam source gives rise to pronounced and overlapping penumbra. Quality Assurance for SRT involves measuring point dose and 2D dose distribution, comparing them with the treatment planning system [4], but hypo-fractionation and small fields prevent the direct use of standard dosimetric methods [7][8]. In this regard, verification by radiochromic film has been widely used to measure the dose profile. However, many factors diminish the accuracy of this approach and make its application less favorable, such as film processing procedure, high cost, no real time feedback, and the unrecyclable nature of the film which raises the cost associated with daily QA. To overcome these challenges, several research groups have investigated the efficiency and applicability of 2D arrays ionization chambers or diode in a clinical setting [3][4][9][10] confirming that the use of 2D electronic array is becoming widespread in radiation therapy.

L'Étourneau *et al.* [11], performs the characterization of a 2D diode array (MapCheck from Sun Nuclear) and observes that the detector is linear, reproducible (SD approximately ± 0.15%), and energy independent. However, dose map calculations in relation to the planning system models show that MapCheck with a detector pitch of 7 mm underestimates dosage gradient of the penumbra region for field sizes smaller than 2 cm due to the layout of the diode array. Studies from Bhardwaj *et al.* and Xu *et al.* [9][12] explore the performances of 2D array of cubic ionization chambers with 5 mm pitch in intensity modulated radiotherapy (IMRT) and Helical

C. S. Porumb, M. Petasecca, M. Newall, A. H. Aldosari, I. Fuduli, P. Metcalfe, M. L. F. Lerch, D. Cutajar, and A. B. Rosenfeld are with the Centre for Medical Radiation Physics, University of Wollongong, NSW 2500, Australia (e-mail: csp528@uow.edu.au; marcop@uow.edu.au; mkn282@uowmail.edu.au; ahaa215@uowmail.edu.au; if473@uowmail.edu.au; metcalfe@uow.edu.au; mlerch@uow.edu.au; deanc@uow.edu.au; anatoly@uow.edu.au).

M. Carolan is with Illawarra Cancer Care Centre, Wollongong Hospital, NSW 2500, Australia (e-mail: Martin.Carolan@sesiahs.health.nsw.gov.au).

V. L. Perevertaylo is with SPA-BIT, Kiev 02232, Ukraine (e-mail: detector@carrier.kiev.ua).

Tomotherapy (a form of IMRT comprised of 'slice-by-slice' delivery of radiation), respectively. The array shows excellent performance in terms of dose distribution reconstruction for regular field size beams (from 4 cm x 4 cm and above) but the authors posit a need to observe care in penumbra region analysis and measurement due to the limited spatial resolutions for the device for smaller field sizes [9][12].

Small field dosimetry requires instrumentation with very high spatial resolution (2 mm pitch or lower) as demonstrated by a study from Aldosari *et al.* [13], combined with a small sensitive volume [14] and a fast readout mechanism to have a real-time feedback. Monolithic silicon detectors represent a valid alternative to achieve such requirements when compared to radiochromic films or ionization chambers [15].

Many other parameters must be considered when using a monolithic silicon detector in radiation therapy as a dosimeter. Silicon detectors reveal a variation in the sensitivity and leakage current with the accumulated dose, as result of radiation damage [13][16][17]. Charge sharing is also of concern for monolithic detector arrays which limits their spatial resolution due to charge drifting in the direction of neighbor electrodes when an event occurs between pixels [18]. Charge sharing effects can be minimized by adjusting the geometry of the pixel, reducing the charge collection time by pre-irradiation of the detector or physically isolating the pixels by grooves [18][19].

Menichelli *et al.* [20] explored the possibility to design a large area monolithic silicon detector for IMRT dosimetry. Despite the excellent performance of the detector in terms of dose linearity, dose rate dependence, and radiation hardness, the array, based on a 2D pixellated p-type epitaxial silicon substrate, has a pitch of 3 mm which makes it inappropriate for small field sizes where the penumbra width can be as small as 2 mm.

Bocci *et al.* [21] explored the use of a single-sided silicon strip detector (SSSSD) placed in a cylindrical phantom in the axial plane (parallel) to the incident beam in IMRT, to be used for 3D dose reconstruction, and found good agreement between the response of the detector, the reference ionization chamber, and Monte Carlo simulations as a function of beam angle. However the detector, which has been designed for high-energy physics, shows inappropriate spatial resolution for use in small-field dosimetry. The disadvantage of the system is the averaging effect due to the strip pitch of 3.1 mm which over-estimates the measurement of the 20%-80% penumbra by more than 55% compared to a reference diode.

This work presents the performance of two monolithic silicon devices designed for measuring dose in a plane for SRT: MagicPlate-512 and DUO array detectors. The sensors are characterized in terms of uniformity, linearity and radiation hardness for use in 6 and 18 MV photon beams.
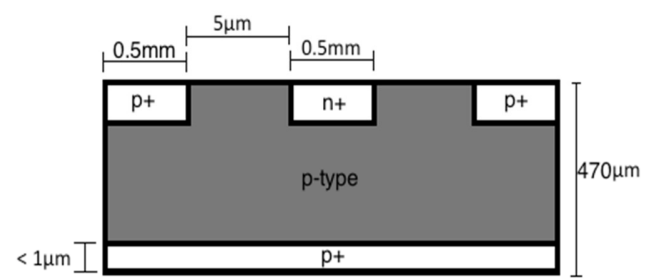
II. MATERIALS AND METHODS
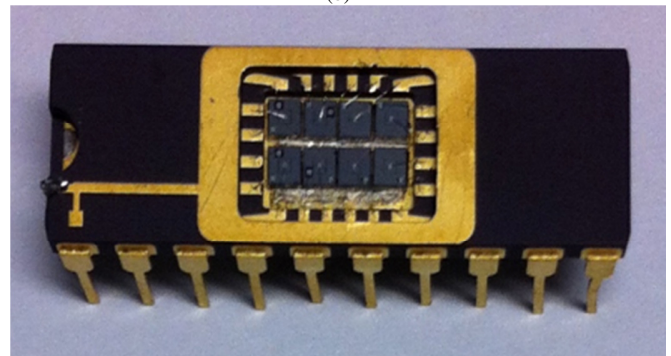
A. *MagicPlate-512*

The MagicPlate-512 detector (MP512; Fig. 1a) is a monolithic dosimeter array of 512 submillimeter size ion
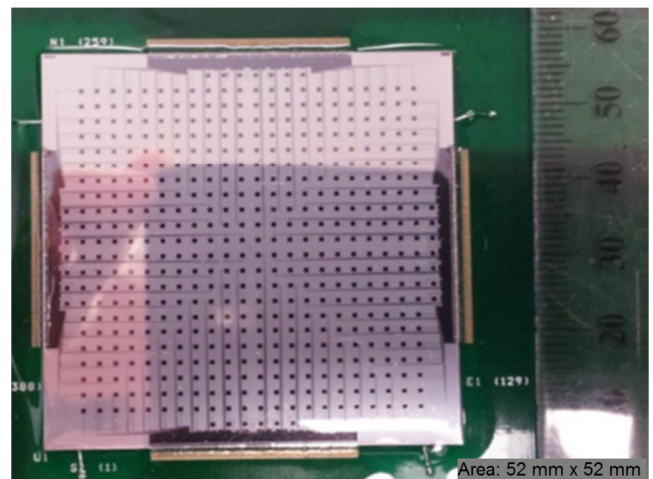
Fig. 1. (a) MP512 array; (b) MP512 single pixel structure diagram (not to scale); (c) MP512 test structures assembled in a dual in line ceramic package

implanted diodes on a p-type silicon substrate, designed by Centre for Medical Radiation Physics (CMRP, Australia) and manufactured at CMRP collaborating microelectronics foundry. Each detector array is manufactured from a single 10.16 cm (4") Czochralski wafer and covers almost entirely the central part of the wafer. The total array area is 52 mm x 52 mm with 2 mm pixel pitch. The silicon detector array, covered by a thin layer (approximately 100 µm) of protective resin epoxy to avoid accidental damage of the connections, is wire bonded to a thin printed circuit board (a 500 µm thick PCB of dimensions 31 cm x 21 cm) which provides the fan-out for connection of the sensor to the readout electronics. The MP512 silicon detector array is operating in photovoltaic mode (no bias applied to the diodes). The pixel elements of the MP512 are produced on 470 µm thick p-Si substrate with an n+ implant of 0.5 mm x 0.5 mm, surrounded by a uniform p+ implant (p-stop) for polarization of the substrate and

isolation of the pixels. The backside of the detector has a similar p+ implant to realize the ohmic back contact and is polarized at the same potential of the front side diode (Fig. 1b). The single pixel test structures were fabricated on the same wafers using different dose of boron ion implantation into a 5 μm gap between n+ and p+ regions to avoid effect of positive charge build-up in a field oxide and changing of size of sensitive volume of n+ implant region with accumulated dose of radiation. Three doping concentrations (Low; Medium; and High level) were adopted for optimization of the manufacturing technology. Fig. 1c shows the diodes' test structures assembled onto a dual in-line (DIL) ceramic package. After the selection of the best configuration of the p-stop doping concentration, the whole detector array has also been tested and performance compared with the test structures' results.

B. MagicPlate DUO

DUO is a monolithic silicon detector with 512 pixels arranged in two orthogonal linear arrays, each with 256 pixels. The DUO was fabricated utilizing similar optimized technology as MP512 (Fig. 2a). The DUO was mounted on an identical circuit board as MP512. The n+ implant size of each pixel is 800 μm long and 20 μm wide, surrounded by p+ region. Similar to MP512, boron ion implantation under the field oxide has been used. The pixels' pitch is 200 μm. Five central pixels create the intersection of the orthogonal arrays; they have an n+ implant area of 200 μm x 200 μm each with pitch 50 μm; and realize a cross-shaped structure in the very center of the detector (Fig. 2b). This small geometry was chosen for the center region of the detector to avoid volumetric effect when performing output factor measurements for small beamlets. The backside of the detector has the same boron implantation as MP512 to produce the ohmic contact. A DUO test structure identical to the array's central cross-shaped pixels and proximal microstrips was used to perform the charge collection efficiency (CCE) study by means of the Ion Beam Induced Charge Collection (IBICC) technique at ANSTO ion microprobe. Full description of IBICC technique can be found at [22].

C. Data Acquisition System

The readout system used to perform the experimental measurements has been developed in-house and is based on the Texas Instruments AFE0064 multichannel electrometer. A field-programmable gate array (FPGA) performs the querying and temporary FIFO storage of the data prior to communicating by a USB 2.0 link with the host and permanently storing the data on the computer. A cross-platform, multi-threaded C++ program named Romulus Radiation Tools was also developed in-house for data decoding, storage, real-time readout of all the pixels, 2D mapping, profiling, and data post-processing and analysis. For further information about the data acquisition system, refer to [23].

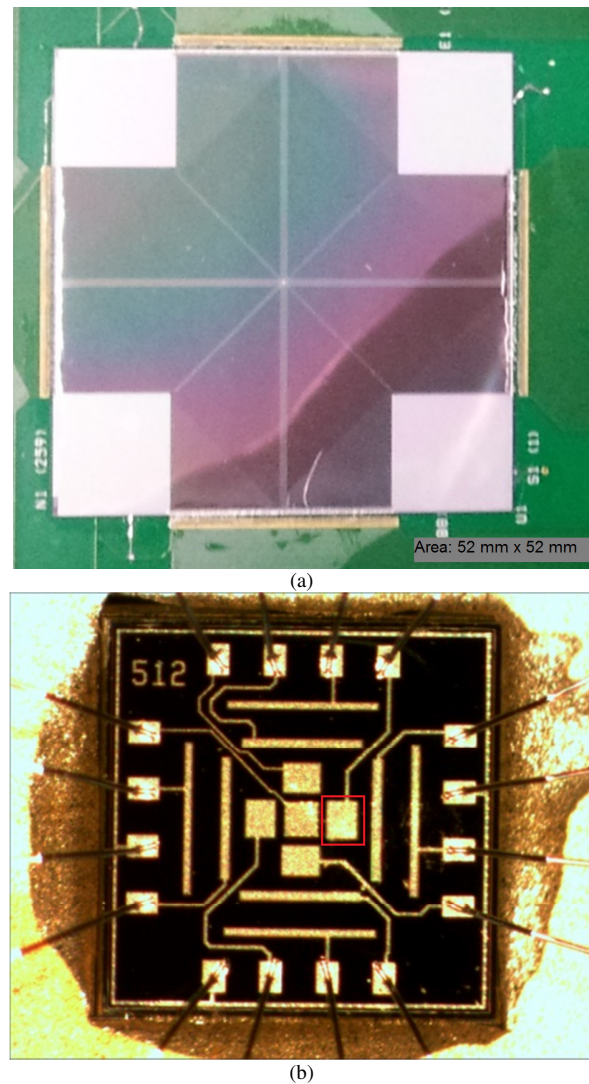Area: 52 mm x 52 mm

(a)

(b)

Fig. 2 (a) DUO whole array; (b) microphotograph of DUO test structure. The red outline shows the pixel which was investigated using IBICC

D. Pre-irradiation Characterization

Current-voltage characteristics of test structures and final detector array were measured prior to, and after irradiation. The measurements were conducted using an automatic Semiconductor Measurement Unit (SMU) 237 from Keithley at a constant laboratory temperature of 24 °C. The detectors' reverse bias was investigated in the range 0 to 50 V. To assess any change after irradiation and the effects of accumulated dose, the current-voltage characteristics were repeated post-irradiation. Capacitance-voltage characteristic was also investigated in the range of 0 V to 50 V reverse bias by the means of the bridge capacitance meter Boonton 7200.

E. Linearity

An ideal dosimeter has perfectly linear response as a function of the dose delivered [21]. To determine linearity, the detectors were irradiated using a medical linac at 'standard conditions', which refers to using a 6 MV linac and placing the detector at 1.5 cm depth in a water equivalent plastic phantom and irradiated by a 10 cm x 10 cm field at 600

MU·min^{-1}, and a Surface to Source Distance (SSD) of 100 cm. In these conditions, 1 MU delivered by the linac corresponds to 1 cGy at depth d_{max} of 1.5 cm. Linearity was measured in increments of 50 cGy in the range 50 MU to 500 MU, and their response plotted against the delivered dose. Response of the detector is provided directly in total charge, as result of the integration of the current in each pixel separately. Integration time is chosen based on the estimated current generated by the beam within the sensitive volume of the detector (500 μm x 500 μm x 100 μm for MP512 and 20 μm x 500 μm x 100 μm for DUO) and the full scale of the dynamic range of the electrometer which is set to 9.6 pC per frame. The system integrates the response from the detector using the linac trigger to synchronize to the pulses and maximize signal-to-noise ratio (SNR). The chosen integration times for maximum readout SNR were 52 μs for MP512 and 100 μs for DUO.

F. Uniformity

The MagicPlate and DUO consist of 512 pixels and the response from each pixel is different due to local substrate defects and parasitic capacitance associated to connections' routing. Additionally, each preamplifier channel has a variation of the gain which can vary within 0.1% to 0.5% of the dynamic range [24]. Hence, the integral dose response of the pixels could be slightly non-uniform. Such non-uniformity can be corrected by irradiating the detectors with a flat field which can be obtained by the means of a medical linac equipped with a flattening filter irradiating the device by 6 MV beam of 20 cm x 20 cm at a depth in water equivalent material of 10 cm, obtaining an equalization factor for each pixel. The equalization factor was obtained by normalizing the response of each individual channel to the flat field (X_i) to the average response of all channels $<X>$, thus generating the equalization factor F_i. To get the data equalized X_{eq-i}, the response of each pixel X_i is normalized by the equalization factor F_i [21] as shown by (1). Three MP512 detector samples with different p-stop implantation concentrations were irradiated and their uniformity analyzed to evaluate their effect on the detector response.

$$F_i = \frac{X_i}{\langle X \rangle}; X_{eq-i} = \frac{X_i}{F_i} \qquad (1)$$

G. Radiation Damage

When exposed to ionizing radiation of any kind, silicon detectors are subject to radiation damage effects of varying severity, depending on the type of incident particles and their energy. These effects act as generation-recombination centers, with equivalent energy levels located in the deep forbidden
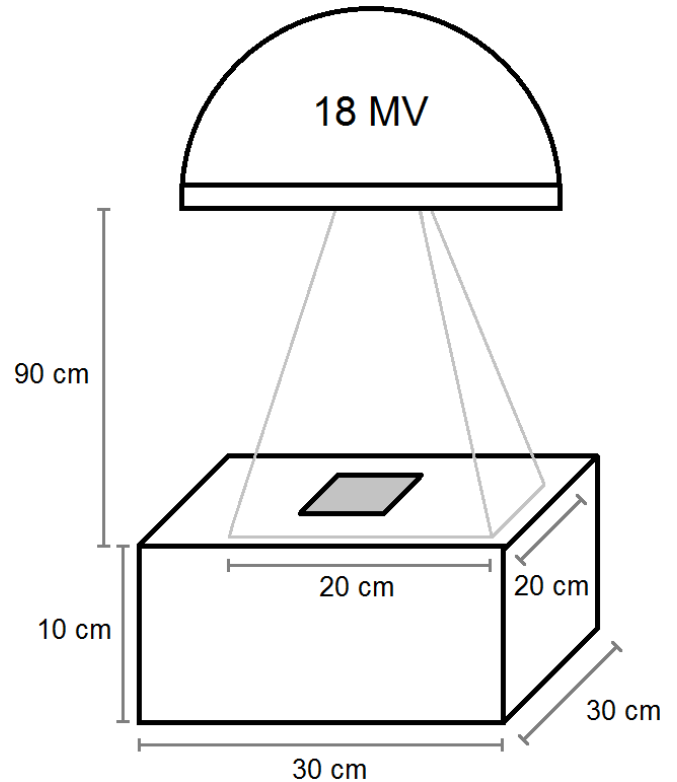

Fig. 3. Schematic diagram of the experimental setup for photoneutron study

gap and hence diminish the detector's sensitivity. It is a requirement of medical radiation detectors to be as stable as possible during their life to avoid frequent and time consuming recalibration procedures. Change in response properties with respect to delivered dose by photon or electron MV energy radiotherapy beams is generally a problem that can be mitigated by delivering a pre-irradiation dose to the detector to stabilize its response. Prior to commencing radiation damage study, the response of the MP512 test structures, as well as the MP512 and DUO arrays, were measured in 'standard conditions'. In this work, photon and photoneutron radiation stability studies were carried out. To induce photon radiation damage, each device was irradiated by a Co-60 gamma source at the Gamma Technology Research Irradiator (GATRI) facility, at the Australian Nuclear Science and Technology Organisation (ANSTO, Australia). MP512 test structures were irradiated up to 40 kGy water equivalent absorbed dose, in steps of 10 kGy. The best manufacturing combination of substrate type and p-stop implantation concentration was chosen based on results obtained with the test structures. Subsequently, the whole MP512 array has been

TABLE I
COMPARISON OF FWHM AND PENUMBRA WIDTH (20%-80%)

FS (cm)	FWHM (mm)			Penumbra (20%-80%) (mm)			Difference FWHM (mm)			Difference Penumbra (mm)		
	0.5	1	2	0.5	1	2	0.5	1	2	0.5	1	2
EBT3	4.73	10.16	20.04	1.85	2.10	2.46						
MP512	5.32	9.88	19.86	2.13	2.67	2.91	-0.60	0.28	0.18	-0.29	-0.57	-0.45
DUO	4.85	9.90	19.87	1.98	2.85	3.38	-0.19	0.35	0.35	-0.37	-0.26	-0.58

The comparison is for MP512 and DUO detectors with respect to EBT3 film; field size is denoted as FS. Statistical uncertainties for the FWHM are less than 2% for DUO and 3.6% for MP512.
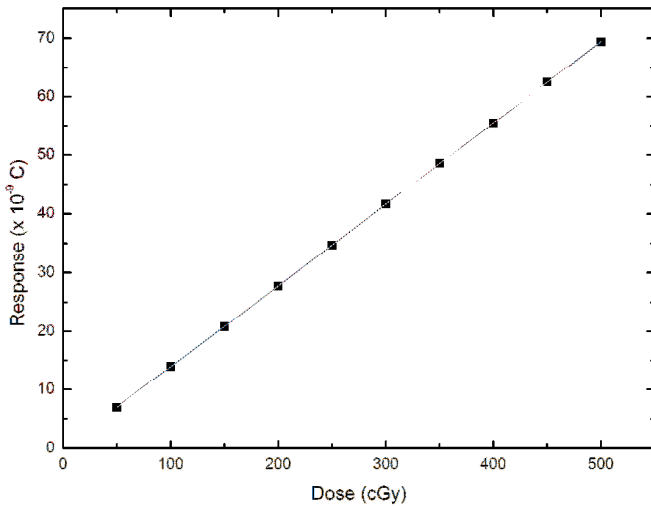
Fig. 4. Linearity response of DUO detector. The adjusted regression coefficient R^2 is 1, the y-intercept is $(1.67 \times 10^{-11} \pm 0.01\%)$ C and the calibration factor is 138.8 pC·cGy^{-1}, which as expected is less than for MP512 quoted in [13]

tested for radiation hardness and results compared with the test structures for validation. DUO array was irradiated up to 140 kGy in steps of 20 kGy. During irradiation, temperature was kept constant at 30 °C and no bias applied, respectively [13].

When a linac with photon energy higher than 10 MV is used, neutrons are produced by photons interacting with high-Z material located in the linac head (primary collimators, jaws, flattening filter) [25][26][27] and any other material surrounding the beam. Neutrons affect the silicon detector response differently than photons, by producing different types of radiation damage, such as displacing of silicon atoms from the crystal lattice and cluster defects [1][27][28]. According to Howell *et al.*, the model and linac manufacturer does not play a role in changing the spectrum and intensity of photo-neutrons [29]. Linacs with energy higher than 10 MV generate primary neutrons with average kinetic energy ranging between 1 and 2 MeV [30][31], with an equivalent dose of 4.5 mSv·Gy^{-1} of photon dose delivered at surface of a solid water phantom [28].

The effect of photo-neutron radiation was investigated using an 18 MV medical Clinac (Varian, USA) at St. George Cancer Centre (Sydney, Australia). The detector, pre-irradiated by 40 kGy of Co-60 gamma photons to stabilize the response variation due to photon damage, was placed at 90 cm SSD at the surface of 10 cm thick solid water backscattering material and irradiated by a beam of 20 cm x 20 cm field size (Fig. 3). To maximize the exposure to neutrons and minimize thermalization, no build-up material was placed on top of the detector. After each irradiation step of approximately 3000 MU at 18 MV (up to a maximum irradiation of 9795 MU corresponding to approximately 300 Gy), the detector response was tested in 'standard conditions' by a 6 MV photon beam.

H. Charge Collection Efficiency, Charge Sharing & Spatial Resolution

To investigate the spatial resolution of the MP512 detector, we used small field photon beams and we looked at the capability to resolve the penumbra of the beam in comparison
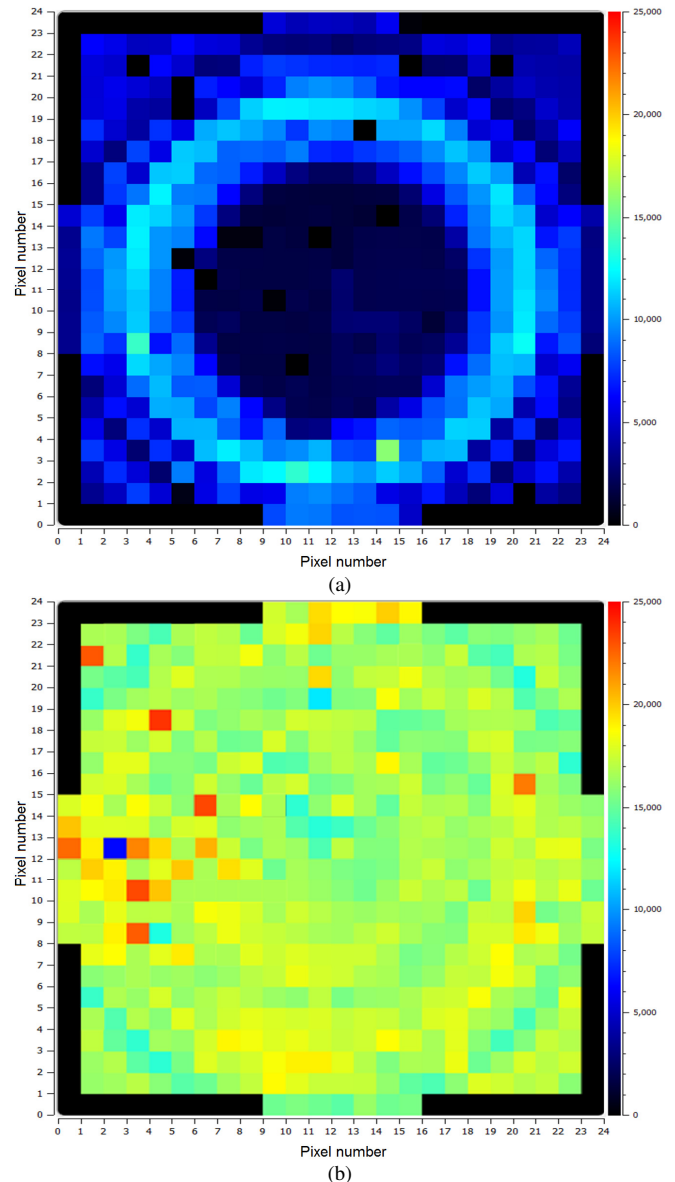

(a)

(b)

Fig. 5. (a) MP512 response map of the samples fabricated with Low p-stop concentration; (b) Response map for sample with High concentration. Colour scale has units of pC, and is normalised to the same value in both maps.

to radiochromic film (Gafchromic EBT3, Ashland, Wayne, NJ). The detector was operated in photovoltaic mode. Photon beams of energy 6 MV and equivalent square sizes of 0.5 cm, 1 cm and 2 cm were used to irradiate both the detectors and EBT3 film at 10 cm depth; 10 cm of solid water backscatter material and a SSD of 100 cm was used. A total dose of 100 cGy has been delivered to achieve a good signal to noise ratio in the film measurements. The film analysis performed in this study is the same adopted by Aldosari *et al.* [13]. Full width at half maximum (FWHM) and 20%-80% studies of the penumbra were performed and compared against the reference EBT3 film.

The DUO detector has a pitch of 200 µm between each pixel. We tested the spatial resolution and charge sharing/collection efficiency of such small pitch detector using small-field photon beams and ion beam induced charge collection (IBICC).
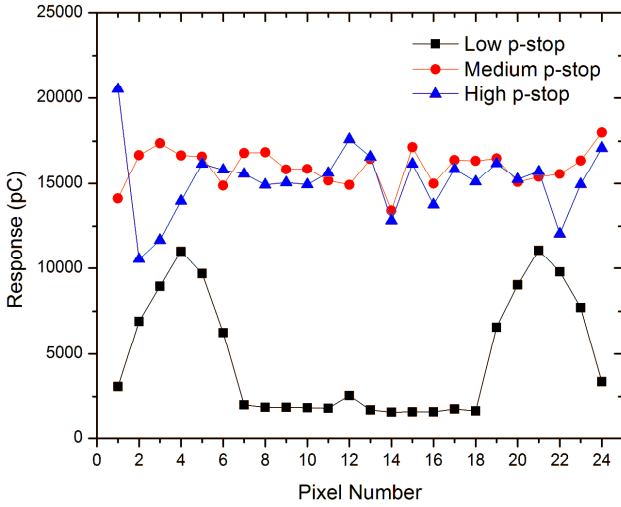
Fig. 6. MP512 vertical profile of the response to a flat field, no equalization. The artifacts are clearly visible on samples with Low p-stop concentration, but less pronounced when Medium and High p-stop is adopted.
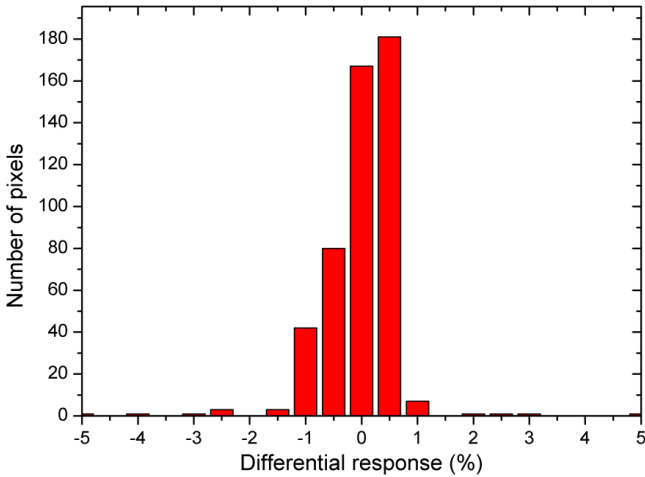

Fig. 7. Statistical distribution of pixel response for DUO manufactured on Cz wafer with High p-stop after equalization.

(a)

(b)

Fig. 8. Variation of the response of DUO (a) and MP512 (b) as a function of the accumulated dose by irradiation with a Co-60 gamma source

Similarly to MP512, the DUO detector was operated in photovoltaic mode, pre-irradiated by Co-60 for stabilization of the response and irradiated by a photon beam in the same experimental conditions comparing the profiles obtained with EBT3 film. The MP512 and DUO are pixelated detectors with a common substrate. Consequently, charge carrier diffusion can lead to a decrease in charge collection efficiency. The IBICC study was performed using the DUO test structures at the ANTARES linear accelerator, Australian Nuclear Science and Technology Organisation, Lucas Heights, Sydney. The He^{2+} ion microbeam of 5.5 MeV with diameter 1 μm was raster-scanned in x-y across the test structure, covering a total area of 1 mm x 1 mm. The central pixels configuration of DUO is composed by five squared pixels, and one of them was chosen as the pixel to be read out by the spectroscopy data acquisition (Fig. 2b); its response was recorded. The response of the pixel and its amplification channel was calibrated against a Hamamatsu PIN diode which acted as the reference detector for evaluation of the full charge collection efficiency (CCE). Charge sharing with adjacent pixels as well as CCE of the test structure was investigated, and energy
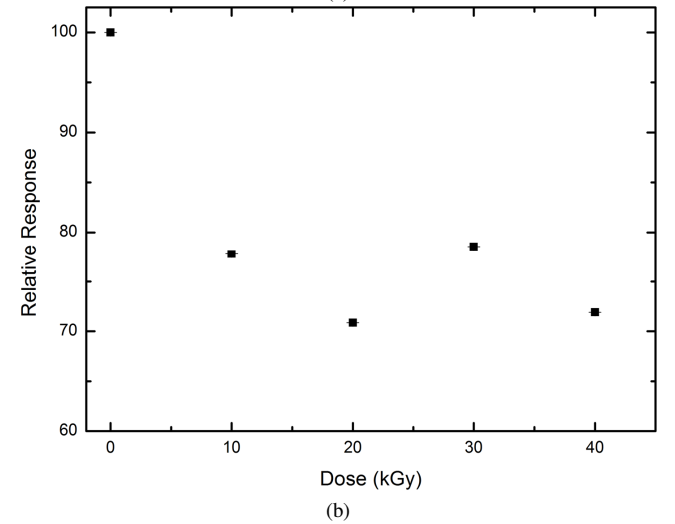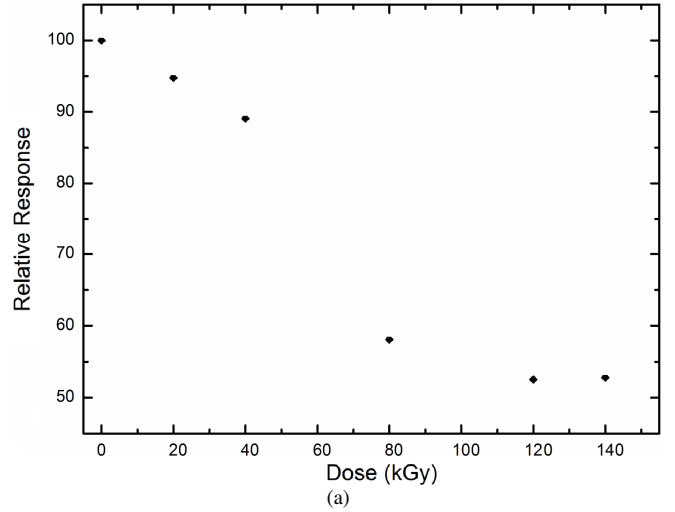
spectra are presented for detector reverse bias of 0 V, 20 V and 40 V. A 2D map of the pixel response and CCE was generated in Matlab (MATHWORKS, US). A dose per pulse dependence (DPP) characterization of MP512 was made for the range 9×10^{-6} to 3.4×10^{-4} Gy/pulse by Aldosari et al. [13]. This was achieved using a field size of 10 cm x 10 cm at 6 MV with a fixed dose rate of 600 MU·min⁻¹ and changing the source to surface distance. The maximum variation obtained was approximately -6% for the lowest dose rate after normalization to the response of the ionization chamber at 2.7 $\times 10^{-4}$ Gy/pulse. The results obtained for MP512 can be extended to the sensor DUO because both the detectors were manufactured using the same fabrication process and the same silicon wafer production batch.

III. RESULTS AND DISCUSSION

A. Pre-irradiation Characterization and Linearity

The current-voltage characteristics of the detector test structures show that the majority of samples undergo breakdown in the range of 45 V to 50 V for both MP512 and DUO test structures. The leakage current is in the order of 10^{-9}
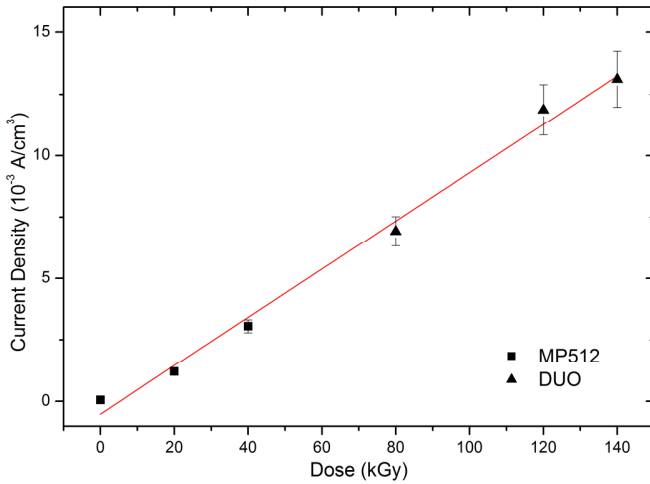
Fig. 9. Variation of the leakage current as a function of the irradiation dose of MP512 and DUO (High p-stop) after normalisation to the detector volume. Error bars are calculated as one standard deviation from the mean value of the current measured in both the detectors for several pixels. The slope of the fit is $(9.83 \pm 0.4) \times 10^{-5} \text{ A·cm}^{-3}\text{·kGy}^{-1}$ and the regression coefficient R^2 is 0.991

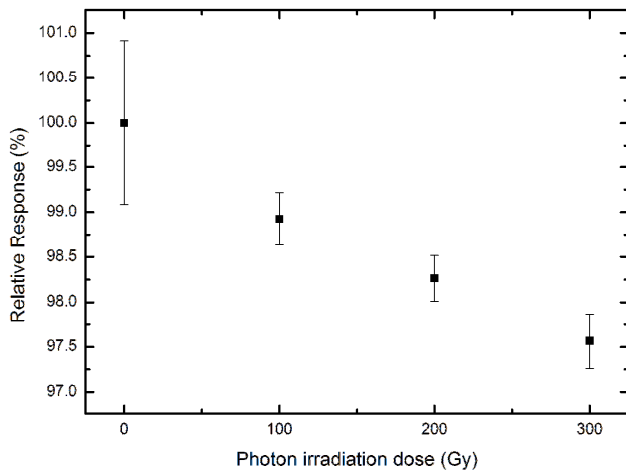Fig. 10. MagicPlate-512 detector response as a function of 18 MV photon irradiation dose A per pixel for 10 V reverse bias.

(a)

(b)

Fig. 11. Profiles reconstructed by MP512 (a), and DUO (b) in comparison with EBT3 film for 0.5 cm up to 2 cm equivalent square field size

The DUO detector demonstrates a good linearity response as a function of dose, as shown in Fig. 4. The calibration factor was calculated to be 138.8 pC·cGy^{-1} with a standard error in slope of $\pm$ (3.2 x 10^{-5}) %. Even with a higher integration time, this calibration factor is smaller than that calculated for MP512, which is 175.2 pC·cGy^{-1} [13]. This is expected due to the smaller sensitive volume of the DUO pixels.

B. Uniformity

MP512 has been fabricated using three different p-stop concentrations (boron doped implant under the field silicon oxide). The p-stop implantation concentration plays a main role not only in the pixel isolation but also in compensating the superficial defects of the substrate, affecting the array response uniformity. When the detector is irradiated by a flat x-ray beam with size of 20 cm x 20 cm within a water equivalent plastic phantom at depth of 10 cm, the sample
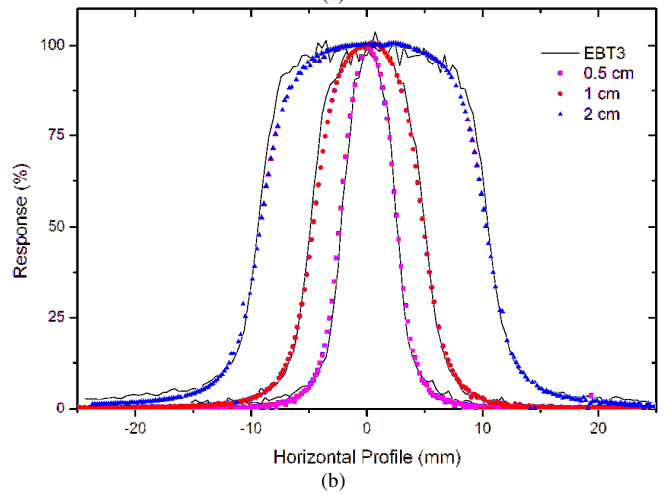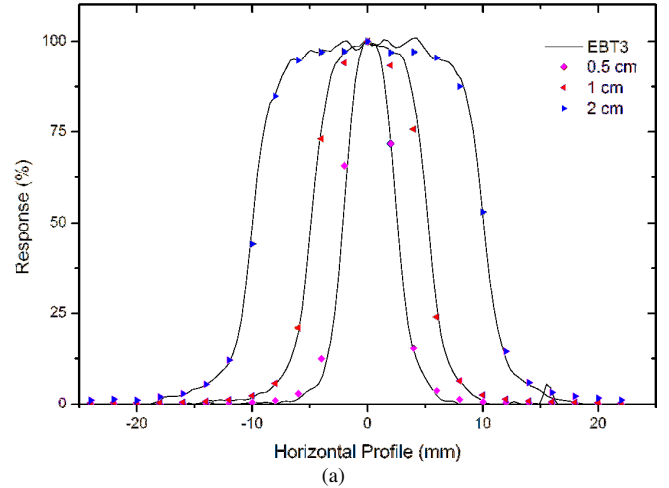
fabricated with Low concentration (Fig. 5a) shows a pronounced non-uniform response across the pixels, in the shape of a ring. Fig. 5b shows, on the same color scale, that a higher p-stop concentration mitigates the non-uniformity. Fig. 6 shows the comparison of the profiles extracted from the flat response of three samples with different p-stop implantation concentration without any equalization.

The variation of the flat field response of the Low p-stop concentration samples is approximately 500% along the ring, and represents a discrepancy which cannot be compensated by the equalization procedure adopted and described in section II.F. The variation for the Medium concentration sample is approximately 9% and can be compensated by the equalization procedure with a final uniformity of the detector response which is within 0.5% for 98% of the pixels as demonstrated in Fig. 6b.

The distribution of the defects across the wafer is normally arranged in rings [32]. Impurities in the substrate in the form of thermal donors may increase the weak electric field, present in photovoltaic mode due to the built-in potential, in proximity of the pixel junction, thus increasing the depletion region and the amount of charge collected by the pixels. A low concentration p-stop implant is not able to compensate for
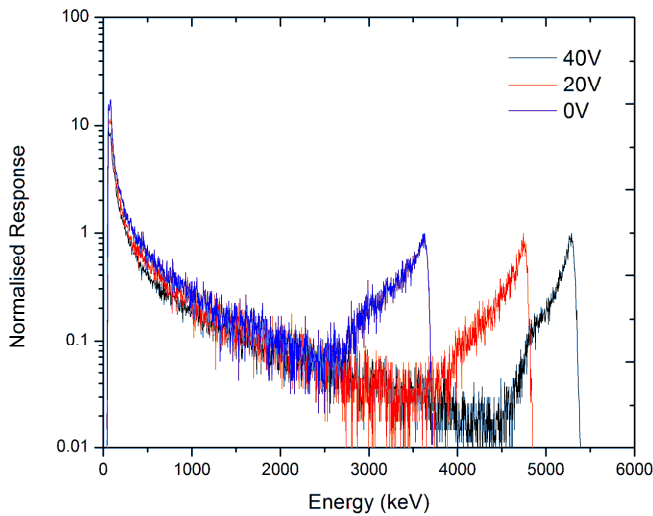
Fig. 12. Spectra of charge collection response for DUO pixel at different reverse bias voltages. The energy of incident alpha particles is 5.5 MeV

such substrate defects in proximity of the pixels which generate the rings on the detector response map when it is irradiated by a uniform photon beam. Moreover, the uniformity of the response improves with higher p-stop concentration because it improves the definition of the active volume around each pixel, particularly in parallel direction to the surface.

Fig. 7 shows that also DUO, when manufactured with High concentration p-stop has a good response's uniformity with 95% of DUO's pixels within 1% of the mean, while over 68% deviate within approximately 0.5%.

C. Radiation Damage

1) Photon Irradiation

In order to obtain a stable response independent of the amount of accumulated dose [33], a pre-irradiation is carried out for the DUO and MP512 detectors (samples with High p-stop). Detectors' sensitivity and response, as a function of delivered dose, is shown in Fig. 8. DUO stabilizes its response within ±2% after irradiation with 120 kGy (dose in water) by a Co-60 gamma photon source (Fig. 8a). The MP512 (High p-stop) shows stabilization of response at doses as low as 20 kGy with a variation of approximately ±5%. Fig. 8b shows that similar results are obtained from the MP512 samples with Medium and High p-stop concentration. Fig. 9 shows the increase [34] of the leakage current density as a function of the accumulated dose for both DUO and MP512 after normalization in respect to the detector volume, and the linear fit calculated which has a slope of 9.83×10^{-5} A·cm^{-3}·kGy^{-1}.

2) Photoneutron Irradiation

Fig. 10 shows the relationship between detector response and 18MV photon irradiation dose; it is clear that the response of the MP512 detector decreases with photoneutron dose at a rate which is approximately 1% per 33 Gy of 18MV photon dose delivered. The direct implication of this result is that when subjected to photoneutron fields, the MP512 detector requires recalibration after about 65 Gy of delivered dose, due to the response of the detector nearing 2% variation.
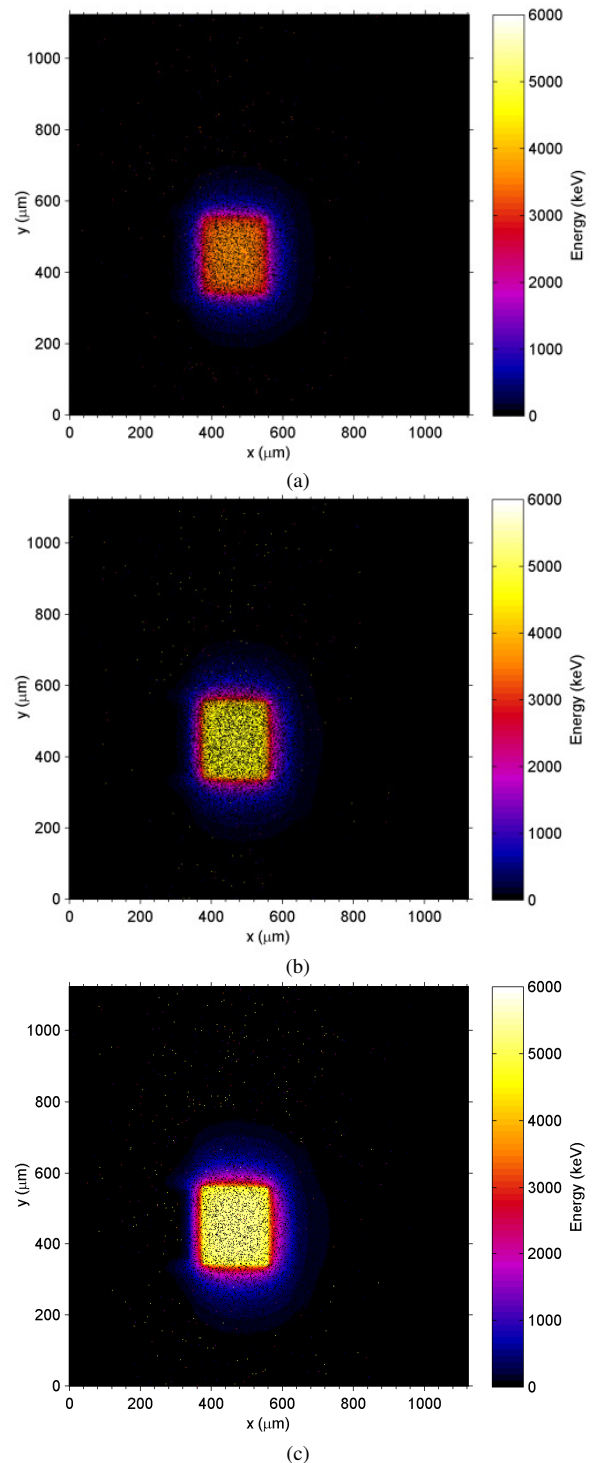
Fig. 13. 2D Map of the collected charge for the DUO inner part; (a) 0 V; (b) 20 V reverse bias; (c) 40 V reverse bias; (d) microphotograph of central section of DUO detector showing the pixel connected to the data acquisition of the Ion Beam Induced Current facility.

D. Charge Collection Efficiency, Charge Sharing & Spatial Resolution

In a monolithic silicon pixelated detector, spatial resolution is not only defined by the pixel pitch and sensitive volume size, but can also be affected by the crosstalk of adjacent pixels. To investigate the DUO's and MP512's effective

spatial resolution, we compared their response to that of radiochromic EBT3 film, which is widely used for dosimetry profiling in hospitals and has the advantage to have a spatial resolution limited by only the capabilities of the optical scanner used to read out the dose distribution. The MP512 and DUO detectors show excellent agreement in comparison with EBT3 film for the three field size penumbrae, as shown in Fig. 11. The variation of the FWHM of the dose profile is up to 0.35 mm for DUO and 0.60 mm for MP512, while the discrepancy for the measurement of the penumbra width (20%-80%) is up to 0.58 mm and 0.57 mm for DUO and MP512, respectively. The results, expressed in mm, are tabulated in Table 1.

The charge collection efficiency and crosstalk of the inner part of the DUO detector has been also investigated by using a 5.5 MeV He^{2+} pencil beam. Alpha particles of this energy have a maximum range in silicon of approximately 28 µm [35]. Fig. 12 shows the energy spectra collected by the DUO test structure pixel for 5.5 MeV alpha particles at three different operating reverse biases: 0 V, 20 V and 40 V. Energy axis is calibrated by using a PIN diode HAMAMATSU (Japan) and the same spectroscopy amplification chain used for the DUO detector. Approximately full CCE (96%) is obtained with the reverse bias of 40V, while for photovoltaic mode 66% of the signal is collected, corresponding to a range in silicon of approximately 16 µm [35]. In the case of 0 V bias, the collection distance (this includes the distance where carriers are drifted by the local electric field and where they diffuse) reaches a depth of only (15 ± 0.5) µm, meaning that as the alpha particles travel through the substrate, any ionizations occurring at a distance larger than the collection distance will not be recorded as signal. This mechanism is responsible also for the charge sharing between pixels.

Fig. 13 shows that the crosstalk between the pixels of DUO is minimal with no charge collected and recorded in adjacent pixels, and approximately less than 20% charge collected outside the n+ junction. This confirms that the DUO detector's spatial resolution is not affected by charge sharing or crosstalk, even with only 200 µm pitch.

IV. CONCLUSIONS

In this work, two novel monolithic dosimeters developed by Centre for Medical Radiation Physics, the DUO and the MP512 detectors, were characterized. We found that the DUO detector presents excellent dose linearity and small statistical variation of pixel response. The pre-irradiation dose required for the stabilization of the response is 120 kGy. DUO spatial resolution and crosstalk have been evaluated by the measurement of a 6MV photon beams of 0.5 cm, 1 cm and 2 cm equivalent square field sizes and compared to EBT3 film. It has been found that FWHM of the reconstructed profile is within 0.35 mm and the penumbra (20%-80%) is within 0.58 mm. Crosstalk between the DUO's pixels is minimal and charge collection efficiency is over 60% even when no bias is applied. The MP512 detector also showed excellent linearity and stabilization of response after pre-irradiation with total dose of 20 kGy. Beam profile reconstruction comparison with EBT3 film shows a discrepancy in FWHM within 0.60 mm

and 20%-80% penumbra within 0.45 mm. Three different detector samples of varying boron implantation charges have been also evaluated to optimize the response of the detector in terms of uniformity and isolation between the pixels. A low p-stop concentration generates a ring artifact with a radius of ~17 mm around the center of the detector due to the silicon wafer manufacturing and residual impurities in the monolithic substrate affecting the rate of recombination of generated electron-hole pairs. This effect can be mitigated by increasing the p-stop concentration up to 100 µC·cm^{-3}. Stability with radiation damage has been also evaluated in a photoneutron field by irradiation by an 18 MV medical linac, where the MP512 detector shows a pronounced decrease of the response as a function of the total irradiation dose. The device requires a recalibration every 65 Gy to account for decrease in response due to cluster defects in the silicon lattice caused by non-thermalized photo-neutrons.

REFERENCES

[1] World health statistics, 2009. [Online]. Available: http://www.who.int/mediacentre/factsheets/fs297/en/index.html [2016 2 10]

[2] A. Aldosari, A. Espinoza, D. Robinson, I. Fuduli, C. Porumb, S. Alshaikh, *et al.*, "Characterization of an innovative p-type epitaxial diode for Dosimetry in modern external beam radiotherapy", *IEEE Trans. Nucl. Sci*, vol 60, no. 6, pp. 4705-4712, 2013

[3] P. A. Jursinic, B. E. Nelms, "A 2-D diode array and analysis software for verification of intensity modulated radiation therapy delivery", *Med. Phys.*, vol. 30, no. 5, pp. 870-879, 2003

[4] J. H. D. Wong, I. Fuduli, M. Carolan, M. Petasecca, M. L. Lerch, V. L. Perevertaylo, *et al.*, "Characterization of a novel two dimensional diode array the 'magic plate' as a radiation detector for radiation therapy treatment", *Med Phys.*, vol. 39, no. 5, pp. 2544-2558, 2012

[5] IAEA (2000). TRS-398 Absorbed Dose Determination in External Beam Radiotherapy: An International Code of Practice for Dosimetry based on Standards of Absorbed Dose to Water. IAEA. Vienna. [Online]. Available: http://www-pub.iaea.org/mtcd/publications/pdf/trs398_scr.pdf [2016 2 10]

[6] P. R. Almond, P. J. Briggs, B. M. Coursey, W. F. Hanson, M. Saiful Huq, R. Nath, *et al.*, "AAPM's TG-51 Protocol for Clinical Reference Dosimetry of High-Energy Photon and Electron Beams", *Med. Phys.*, vol. 26, no. 9, pp 1847-1870, Sep. 1999

[7] T. S. A. Underwood, H. C. Winter, M. A. Hill, J. D. Fenwick, "Detector density and small field dosimetry: Integral versus point dose measurement schemes", *Med. Phys.*, vol. 40, no. 8, Aug. 2013

[8] I. J. Das, G. X. Ding, A. Ahnesjö, "Small fields: Nonequilibrium radiation dosimetry" *Med. Phys.*, vol. 35, no. 1, pp. 206-215, 2008

[9] A. K. Bhardwaj, S. C. Sharma, B. Rana, A. Shukla, "Study of 2D ion chamber array for angular response and QA of dynamic MLC and pretreatment IMRT plans", *Reports of Practical Oncology & Radiotherapy*, vol. 14, no. 3, pp. 89-94, 2009

[10] S. Cilla, L. Grimaldi, G. D'Onofrio, P. Viola, M. Craus, L. Azario, et al., "Portal dose measurements by a 2D array", *Physica medica: official journal of the Italian Association of Biomedical Physics (AIFB)*, vol. 23, no. 1, pp. 25-32, 2007

[11] D. L'Étourneau, M. Gulam, D. Yan, M. Oldham. J. W. Wong, "Evaluation of a 2D diode array for IMRT quality assurance", *Radiotherapy and Oncology*, vol. 70, no. 2, pp. 199-206, 2004

[12] S. Xu, C. Xie, Z. Ju, X. Dai, H. Gong, L. Wang, *et al.*, "Dose verification of helical tomotherapy intensity modulated radiation therapy planning using 2D-array ion chambers", *Biomedical Imaging and Intervention Journal*, vol. 6, no. 2 pp. e24-e24, 2010

[13] A. H. Aldosari, M. Petasecca, A. Espinoza, M. Newall, I. Fuduli, C. Porumb, *et al.*, "A two dimensional silicon detectors array for quality assurance in stereotactic radiotherapy: MagicPlate-512", *Med. Phys.*, vol. 41, no. 9, Sept. 2014

[14] A. B. Rosenfeld, "Electronic dosimetry in radiation therapy", *Rad. Meas.*, vol. 41, pp. S134-S153, 2007

[15] B. Nilsson, B.-I. Rudén, B. Sorcini, "Characteristics of silicon diodes as patient dosemeters in external radiation therapy", *Radiotherapy and Oncology*, vol. 11, no. 3, pp. 279-288, 1988

[16] M. Petasecca, M. K. Newall, J. T. Booth, M. Duncan, A. H. Aldosari, I. Fuduli, *et al.*, MagicPlate-512: "A 2D silicon detector array for quality assurance of stereotactic motion adaptive radiotherapy", *Med. Phys.*, vol. 42, no. 6, pp. 2992-3004, 2015

[17] D. Wilkins, X. A. Li, J. Cygler, L. Gerig, "The effect of dose rate dependence of p-type silicon detectors on linac relative dosimetry", *Med. Phys.*, vol. 24, no. 6 pp. 879-881, 1997

[18] P. Maj, A. Baumbaugh, G. Deptuch, P. Grybos, R. Szczygiel, "Algorithms for minimization of charge sharing effects in a hybrid pixel detector taking into account hardware limitations in deep submicron technology", *JINST*, vol. 7, 2012

[19] L. Tlustos, M. Campbell, E. Heijne, X. Llopart, "Signal variations in high-granularity Si pixel detectors", *IEEE Trans. Nucl. Sci.*, vol. 51, no. 6, pp. 3006-3012, 2004

[20] D. Menichelli, M. Bruzzi, M. Bucciolini, C. Talamonti, M. Casati, L. Marrazzo, *et al.*, "Design and development of a silicon-segmented detector for 2D dose measurements in radiotherapy", *Nucl. Instr. Meth. A*, vol. 583, pp. 109–113, 2007

[21] A. Bocci, M. A. Cortes-Giraldo, M. I. Gallardo, J. M. Espino, R. Arráns, M. A. G. Alvarez, *et al.*, "Silicon strip detector for a novel 2D dosimetric method for radiotherapy treatment verification", *Nuclear Instruments and Methods A*, vol. 673, pp.98–106, 2012

[22] L. T. Tran, L. Chartier, D. A. Prokopovich, M. I. Reinhard, M. Petasecca, S. Guatelli, *et al.*, "3D-Mesa 'Bridge' silicon microdosimeter: charge collection study and application to RBE studies in 12C radiation therapy", *IEEE Trans. Nucl. Sci.*, vol. 62, no. 2, pp. 504-511, 2015

[23] I. Fuduli, M. K. Newall, A. A. Espinoza, C. S. Porumb, M. Carolan, M. L. F. Lerch, *et al.*, "Multichannel data acquisition system comparison for quality assurance in external beam radiation therapy", *Rad. Meas.*, vol. 76, no. 1, pp. 338-341, 2014

[24] Texas Instruments. (2009). 64 Channel Analog Front End for Digital X-Ray Detector. [Online.]. Available: http://www.ti.com/lit/ds/symlink/afe0064.pdf [2016 2 10]

[25] A. Facure, R. C. Falcão, A. X. Silva, V. R. Crispim, J. C. Vitorelli, "A study of neutron spectra from medical linear accelerators", *Applied radiation and isotopes : including data, instrumentation and methods for use in agriculture, industry and medicine*, vol. 62, no. 1, pp. 69-72, 2005

[26] L. Paredes, R. Genis, M. Balcázar, L. Tavera, E. Camacho, "Fast neutron leakage in 18 MeV medical electron accelerator", *Rad. Meas.*, vol. 31, no. 1–6, pp. 475-478, 1999

[27] F. S. Kry, R. M. Howell, M. Salehpour, D. S. Followill, "Neutron spectra and dose equivalents calculated in tissue for high-energy radiation therapy", *Med. Phys.*, vol. 36, no. 4, pp. 1244-1250, 2009

[28] F. d'Errico, R. Nath, L. Tana, G. Curzio, W. G. Alberts, "In-phantom dosimetry and spectrometry of photoneutrons from an 18 MV linear accelerator", *Med. Phys.*, vol. 25, no. 9, pp. 1717-1724, 1998

[29] R. M. Howell, S. F. Kry, E. Burgett, N. E. Hertel, D. S. Followill, "Secondary neutron spectra from modern Varian, Siemens, and Elekta linacs with multileaf collimators", *Med. Phys.*, vol. 36, no. 9, pp. 4027-4038, 2009

[30] S. R. Chester, R.-M. Renate, M. Leon, "In vivo and phantom measurements of the secondary photon and neutron doses for prostate patients undergoing 18 MV IMRT", *Med. Phys.*, vol. 33, no. 10, pp. 3734-3742, 2006

[31] F. d'Errico, M. Luszik-Bhadra, R. Nath, B. R. Siebert, U. Wolf, "Depth dose-equivalent and effective energies of photoneutrons generated by 6-18 MV x-ray beams for radiotherapy", *Health Physics*, vol. 80, no. 1, pp. 4-11, 2001

[32] S. M. Sze, K. K. Ng, "Physics of Semiconductor Devices", 3rd ed., Wiley

[33] G. Rikner, E. Grusell, "General specifications for silicon semiconductors for use in radiation dosimetry", *Phys. Med. Biol.*, vol. 32, no. 9, p. 1109, 1987

[34] Z. Li, H. W. Kraner, "Fast neutron radiation damage effects on high resistivity silicon junction detectors", *J. Electronic Materials*, vol. 21, no. 7, pp. 701-705, 1992

[35] J. Ziegler. (2015). SRIM software. [Online]. Available: http://www.srim.org/ [2016 2 10]

[36] S. Venkataraman, K. E. Malkoske, M. Jensen, K. D. Nakonechny, G. Asuni, B. M. C. McCurdy, "The influence of a novel transmission detector on 6 MV x-ray beam characteristics", *Phys. Med. Biol.*, vol. 54, no. 10, pp. 3173-3183, 2009

[37] S. J. Moloi, M. McPherson, "Current–voltage behaviour of Schottky diodes fabricated on p-type silicon for radiation hard detectors", *Physica B: Condensed Matter*, vol. 404, no. 16, pp. 2251-2258, 2009

[38] G. Mazza, R. Cirio, M. Donetti, A. La Rosa, A. Luparia, F. Marchetto, *et al.*, "A 64-channel wide dynamic range charge measurement ASIC for strip and pixel ionization detectors", *IEEE Trans. Nucl. Sci.*, vol. 52, no. 4, pp. 847-853, 2005

[39] M. Bruzzi, M. Bucciolini, M. Casati, D. Menichelli, C. Talamonti, C. Piemonte, *et al.*, "Epitaxial silicon devices for dosimetry applications", *Applied Physics Letters*, vol. 90, no. 17, p. 172109, 2007

[40] M. Petasecca, F. Moscatelli, D. Passeri, G. U. Pignatel, "Numerical simulation of radiation damage effects in p-type silicon detectors", *Nuclear Inst. and Methods in Physics Research, A*, vol. 563, no. 1, pp. 192-195, 2006

[41] X. R. Zhu, "Entrance dose measurements for in-vivo diode dosimetry: Comparison of correction factors for two types of commercial silicon diode detectors", *Journal of Applied Clinical Medical Physics*, vol. 1, no. 3, pp. 100-107, 2008

[42] N. Jornet, M. Ribas, T. Eudaldo, "In vivo dosimetry: Intercomparison between p-type based and n-type based diodes for the 16–25 MV energy range", *Med. Phys.*, vol. 27, no. 6, pp. 1287-1293, 2000